# Photochemistry of aqueous C60 clusters: evidence of 1O2 formation and its role in mediating C60 phototransformation.

2 AUTHORS:

Wen-Che Hou
National Cheng Kung University
**16** PUBLICATIONS **383** CITATIONS

SEE PROFILE

Chad T Jafvert
Purdue University
**103** PUBLICATIONS **2,382** CITATIONS

SEE PROFILE

# Photochemistry of Aqueous C$_{60}$ Clusters: Evidence of $^1O_2$ Formation and its Role in Mediating C$_{60}$ Phototransformation

W E N - C H E   H O U   A N D   C H A D   T .   J A F V E R T *

*Purdue University, School of Civil Engineering; West Lafayette, Indiana 47907*

The expected rapid expansion of nanotechnology industries has raised concern over the environmental fate and effects of materials created by these industries, including carbon-based fullerenes. In this study, the reaction mechanism responsible for the photochemical transformation of aqueous C$_{60}$ clusters (nC$_{60}$) in sunlight has been examined. Evidence is presented that under lamps that emit light only within the solar spectrum, $^1O_2$ is produced via aqueous nC$_{60}$ suspensions, using furfuryl alcohol (FFA) as an indicator. In air-equilibrated suspensions, the losses of 0.2 mM FFA and 0.8 mg/L C$_{60}$ were >90% and 70% after 15 h, while removing oxygen, the precursor of $^1O_2$, stopped both reactions, indicating that $^1O_2$ was produced and mediated nC$_{60}$ phototransformation. Similar reactions performed in deuterium oxide and with added azide ion resulted in accelerated and slowed loss of FFA, respectively, as expected if $^1O_2$ is a reaction intermediate. $^1O_2$ production (as measured by FFA loss) increased with time as more water-soluble intermediate products accumulated in solution. In summer sunlight (West Lafayette, IN, 86° 55′ W, 40° 26′ N), suspensions of 5 mg/L nC$_{60}$ produced $^1O_2$ concentrations 1 order of magnitude higher than the average value typically found in natural waters containing the same mass of natural organic carbon.

## Introduction

C$_{60}$ and other carbon-based nanomaterials have attracted considerable attention due to their unique properties, making their widespread use in many commercial products a potential reality (*1*), with the caveat that such uses must be environmentally sustainable. However, at this point in time, little is known about their potential impacts on the environment including their persistence and toxicity (*2, 3*). Although C$_{60}$'s aqueous solubility has been reported to be low at 2.6−8.0 ng/L (*4*), it is well-known that C$_{60}$ forms stable clusters (nC$_{60}$) upon mixing with water (*5*). While the transport and toxicity of nC$_{60}$ have been intensively investigated, knowledge regarding reactivity in the aquatic environment, including photoreactivity, is limited.

There are two types of photochemical pathways (*6*) that C$_{60}$ can undergo, each generating different reactive oxygen species (ROS). The *Type I* pathway leads to electron transfer where photoexcited singlet C$_{60}$ ($^1$C$_{60}$) rapidly transitions to triplet C$_{60}$ ($^3$C$_{60}$) that is more electronegative (*7*) and can accept an electron from donors, forming C$_{60}$$^{\cdot-}$. Subsequently, the

superoxide anion radical (O$_2$$^{\cdot-}$) can form via O$_2$ receiving the electron from C$_{60}$$^{\cdot-}$. For the *Type I* pathway to occur, an electron donor is required: This is the case under physiological conditions where the in vivo reductant NADH is available, potentially leading to DNA cleavage (*8*). The *Type II* pathway, which is evident in this study, has been reviewed in our earlier work (*9*) and involves energy transfer from photoexcited $^3$C$_{60}$ to O$_2$, forming singlet oxygen ($^1O_2$).

C$_{60}$ is an efficient photosensitizer for $^1O_2$ production with a high quantum yield in nonpolar organic solvents (*10*). However, conflicting results have been reported in the literature when the C$_{60}$ is in cluster form in the aqueous phase. In studies by Lee et al. (*11, 12*) and Hotze et al. (*13*), using electron paramagnetic resonance (EPR) coupled with spin trapping reagents to detect $^1O_2$, or using furfuryl alcohol (FFA) as a $^1O_2$ scavenger, no detectable $^1O_2$ production occurred in aqueous nC$_{60}$ solution within 2 h of irradiation at $\lambda = 300-400$ nm. It was claimed that $^3$C$_{60}$, a key species in mediating $^1O_2$ production, is rapidly quenched by neighboring C$_{60}$ molecules in the clusters (*12*). In contrast, using another technique, Bilski et al. (*14*) were able to detect $^1O_2$ produced from nC$_{60}$ based on its phosphorescence at $\lambda = 1250-1330$ nm on exposure to light at 366 nm. Our earlier paper (*9*) has demonstrated that phototransformation of nC$_{60}$ occurs in sunlight and O$_2$ plays an important role. Other studies (*15, 16*) also have indicated that the oxidative phototransformation of C$_{60}$ in organic solvents requires the reaction of $^1O_2$ with $^3$C$_{60}$. Information on the role that the species $^1O_2$ plays in the phototransformation of nC$_{60}$ in the aqueous phase is limited as no previous study has reported on $^1O_2$ production by nC$_{60}$ in sunlight.

$^1O_2$ is a ROS that has environmental and biological implications. It is widely known that sunlit waters containing dissolved organic matter (DOM) generate $^1O_2$ (*17, 18*). $^1O_2$ produced via aqueous DOM has been reported to affect other aquatic processes including pollutant removal (*19*). Bioassays in the presence of C$_{60}$ or its derivatives under lamp light indicate DNA cleavage (*20*) and oxidative damage to rat liver cells occurs (*21*). It has been suggested that ROS including $^1O_2$ induce these damages. While these results represent a potential hazard of C$_{60}$ in vitro under artificial light, it is uncertain how significant similar biological responses will be in natural systems where C$_{60}$ is present. Due to its extreme hydrophobicity (*4*), the thermodynamic potential exists for molecular C$_{60}$ to occur within biological materials at significant concentrations; however, nC$_{60}$ aggregates are the form that may occur at high concentrations within water. Quantifying $^1O_2$ production during aqueous nC$_{60}$ phototransformation may be an important element for assessing the potential environmental impacts of C$_{60}$.

In this study, we provide evidence that formation of $^1O_2$ occurs during irradiation of aqueous nC$_{60}$ at wavelengths within the solar spectrum ($\lambda = 350 \pm 50$ nm) using FFA as an indicator. Additional evidence includes the decrease in dissolved O$_2$ concentration during nC$_{60}$ phototransformation, and the systematic $^1O_2$ production trends that occurred in the presence of deuterium oxide (D$_2$O) and azide ion. The role of potential impurities in the solution phase derived during nC$_{60}$ preparation by solvent transfer (*3*) in contributing to photoreactivity was ruled out by testing the aqueous phase where nC$_{60}$ was removed and by washing nC$_{60}$ aggregates repeatedly before irradiation. Additional experiments were performed with nC$_{60}$ prepared by mixing pure C$_{60}$ and pure water. Experiments under sunlight were performed to estimate the rate of $^1O_2$ production via nC$_{60}$ in natural surface waters. As our experiments indicate, it is likely that $^1O_2$ is

produced from $O_2$ by excited-state $C_{60}$, and then reacts with $^3C_{60}$ to form intermediate products that can absorb additional photons, producing more triplet-state carbon and additional $^1O_2$.

## Materials and Methods

**Chemicals.** Sources of chemicals and $C_{60}$ solution preparation procedures are provided in the Supporting Information (SI).

**Cluster Characterization.** Cluster size was measured at 25 °C by dynamic light scattering (DLS) with a DynaPro 99 particle size analyzer (Wyatt Technology Corp., Santa Barbara, CA). All UV−visible absorption spectra were recorded with a Varian Cary 300 Biospectrophotometer with matched 1-cm path-length quartz cuvettes.

**$^1O_2$ Measurement.** $^1O_2$ production was monitored by the loss of furfuryl alcohol (FFA) (22). The reaction of $^1O_2$ and FFA is independent of pH = 5−12 (23). The rate law for FFA reacting with $^1O_2$ has been described previously (18)

$$-\frac{d[\text{FFA}]}{dt} = k_r[^1O_2]_{ss}[\text{FFA}] \quad (1)$$

$$-\frac{d[\text{FFA}]}{dt} = k_{obs}[\text{FFA}] \quad (2)$$

$$[^1O_2]_{ss} = \frac{k_{obs}}{k_r} \quad (3)$$

where $[^1O_2]_{ss}$ is the steady-state concentration of $^1O_2$, $k_{obs}$ is the experimentally derived pseudo first-order rate constant, and $k_r = 1.2 \times 10^8$ $M^{-1}s^{-1}$ (22). The steady-state assumption on $[^1O_2]$ is generally invoked to estimate its concentration in sunlit natural waters as a constant sensitizer concentration can be assumed (18). To maintain loss of FFA as first-order and to prevent suppression of $[^1O_2]_{ss}$, it is necessary to limit [FFA] < 0.2 mM (18). Comparing eqs 1 and 2 reveals that $[^1O_2]_{ss}$ can be obtained by dividing $k_{obs}$ by $k_r$ (eq 3).

In our experiments where $C_{60}$ within $nC_{60}$ clusters is the sensitizer, the concentration of molecular $C_{60}$ (normalized to the aqueous volume) decreased to less than 60% of the initial concentration during irradiation. As a result, the kinetics of FFA loss do not appear first-order (see below), and the assumption of steady-state concentration on $^1O_2$ does not apply. Hence, the $[^1O_2]$ concentration with time was evaluated by

$$[^1O_2]_t = \frac{-\frac{d[\text{FFA}]}{dt}t}{k_r[\text{FFA}]_t} \quad (4)$$

where $[^1O_2]_t$, $-d[\text{FFA}]/dt_t$, and $[\text{FFA}]_t$ are the average $^1O_2$ concentration, FFA degradation rate, and FFA concentration, respectively, between two sampling points over time. $^1O_2$ concentrations evaluated with eqs 3 and 4 reveal comparable results (see below). The light screening factor ($S_\lambda$) that considers light attenuation through the sample and converts bulk $[^1O_2]$ to the surface value $([^1O_2]^0)$ is given by eqs 5 and 6 (18, 24)

$$S_\lambda = \frac{1 - 10^{-\varepsilon_\lambda Cl}}{2.303\varepsilon_\lambda Cl} \quad (5)$$

$$[^1O_2]^0 = \frac{[^1O_2]}{S_\lambda} \quad (6)$$

where $\varepsilon_\lambda$ is the light attenuation coefficient of the sensitizer (i.e., $nC_{60}$) at wavelength $\lambda$, which for $nC_{60}$ includes both light absorption and effects of particle light scattering, and hence is not a true molar extinction coefficient. Because $nC_{60}$ cluster solutions display a broad light attenuation "spectra" from
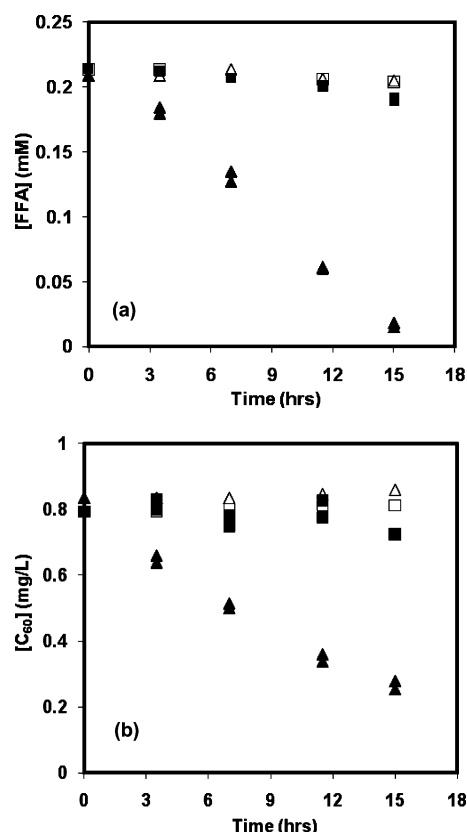


**FIGURE 1.** Irradiation of 0.8 mg/L $nC_{60}$ with 0.2 mM FFA at pH = 7 in lamp light, showing (a) FFA and (b) $C_{60}$ measured in deoxygenated samples (■), air-equilibrated samples (▲), and dark control samples [deoxygenated (□) and air-equilibrated (△)].

300−800 nm, $\varepsilon_\lambda$ was determined at $\lambda = 400$ nm where sunlight emits the highest energy. $C$ is the $C_{60}$ concentration and $l$ is the effective path length, approximated by the geometric-average path length of the tube at 1.26 cm, which is close to that used in a similar study (18).

**Irradiation.** Irradiations were performed with lamps that emit only in the solar spectrum from 300−410 nm, centered at 350 nm, or in sunlight. The description of the photochemical apparatus, experiment procedures, and the acquisition of solar intensity data can be found in our previous paper (9).

**Analysis.** $C_{60}$ was quantified by HPLC methods described previously (9). For FFA measurement in samples containing $nC_{60}$, a portion (5 mL) was centrifuged at 13,000$g$ for 1 h prior to analyzing the supernatant by HPLC. Samples without $nC_{60}$ were analyzed directly by HPLC. Chromatography of FFA occurred on a 150 mm × 4.6 mm Supelcosil LC-PAH column with a mobile phase of 1:1 (v:v) methanol/water at 1 mL/min, and UV-absorbance detection at 219 nm.

## Results and Discussion

Initial experiments were performed in lamp light that has the advantage of a relatively constant and high energy output to examine production of $^1O_2$. The UV−visible spectra of $C_{60}$ clusters and the light emitted by the lamps and sunlight are similar to those reported previously (9). Figure 1a reports the loss of 0.2 mM FFA sensitized by 0.8 mg/L $nC_{60}$ in lamp light with and without dissolved $O_2$. After 15 h of irradiation, FFA loss was >90% in the air-equilibrated $nC_{60}$ samples whereas loss in the deoxygenated samples was insignificant (<10%), indicating $O_2$ plays a large role in the degradation of FFA. Both light and $nC_{60}$ are required, as the dark control
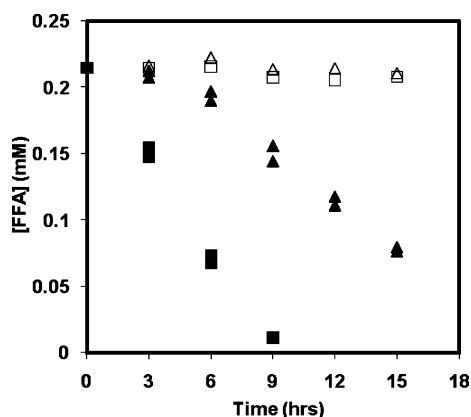
**FIGURE 2.** FFA loss at pH 7 under lamp light in 0.73 mg/L $nC_{60}$ prepared in $D_2O$ (■) and in $H_2O$ (▲), and in the corresponding dark control samples [$D_2O$ (□) and $H_2O$ (△)].

samples and the irradiated samples containing only FFA (data not shown) revealed no decay of FFA. The slight loss of FFA in the deoxygenated samples may be attributed to residual oxygen or the direct reaction of FFA with excited $C_{60}$. These findings are suggestive that $^1O_2$ was produced, as eliminating $O_2$, the precursor of $^1O_2$ that subsequently reacts with the substrate (i.e., FFA), leads to a significant decrease in FFA loss. Recently, Bilski et al. (*14*) have detected $^1O_2$ produced by irradiating aqueous $nC_{60}$ at 366 nm based on $^1O_2$'s characteristic phosphorescence at $\lambda = 1250-1330$ nm. In their study, $^1O_2$ phosphorescence was sensitive to $O_2$ concentration and completely disappeared in saturated $N_2$ solutions, consistent with our result using FFA as an indicator.

In the same experiment shown in Figure 1a, $C_{60}$ loss was measured and is reported in Figure 1b. The $C_{60}$ loss was almost completely quenched in the deoxygenated samples in the presence of FFA as a $^1O_2$ scavenger. This confirms our earlier work (*9*) that $^1O_2$ plays a role in the phototransformation of aqueous $C_{60}$ clusters. In the air-equilibrated samples, the FFA loss due to the reaction with $^1O_2$ only accounts for a portion of $^1O_2$ generated in the system, as $^1O_2$ also reacts with $C_{60}$ as indicated by $C_{60}$ loss in the aerated samples.

To further confirm production of $^1O_2$, similar $nC_{60}$ clusters dispersed in $D_2O$ and in $H_2O$ were irradiated (Figure 2). $D_2O$ quenches $^1O_2$ at a slower rate than $H_2O$ ($k_d$ ($D_2O$) = $1.6 \times 10^4$ s$^{-1}$; $k_d$ ($H_2O$) = $2.5 \times 10^5$ s$^{-1}$) (*25*). Whereas FFA loss was 64% in $H_2O$ after 15 h of irradiation, FFA loss was 95% in $D_2O$ after 9 h, again suggesting involvement of $^1O_2$. In contrast, Bilski et al. (*14*) demonstrated that the $^1O_2$ lifetime ($\sim 3 \mu$s) based on its phosphorescence decay was the same for $nC_{60}$ in $H_2O$ and $D_2O$. It was suggested that the phosphorescence was not from $^1O_2$ in the bulk phase, but from $^1O_2$ within the $nC_{60}$ nanocrystals, leading to the solvent-independent lifetime. The photochemical reaction of $nC_{60}$ is a dynamic process where $^1O_2$ even reacts with the photosensitizer $C_{60}$. Considering that $C_{60}$ decayed 42% and 44% in the same $D_2O$ and $H_2O$ experiments, respectively, in 9 h (data not shown), it is likely that, in addition to bulk and nanocrystal phase $^1O_2$ reacting with $nC_{60}$, the water-soluble $C_{60}$ photoproducts (*9*) also induced $^1O_2$ production, resulting in the differential loss rates of FFA in $D_2O$ and $H_2O$. The small difference in $C_{60}$ loss from $nC_{60}$ in $D_2O$ and $H_2O$ suggests that another important species, $^3C_{60}$, is mediating (i.e., limiting) phototransformation of $nC_{60}$ in addition to $^1O_2$, otherwise the $C_{60}$ loss would have appeared autocatalytic instead of first order (see below). It is noted that $C_{60}$ aqueous aggregates used for this experiment were washed 3 times by repeated centrifugation and resuspension and then diluted to the target concentration to minimize the interference of solvent residues (*3*). In addition, experiments (data not shown) were performed with $nC_{60}$
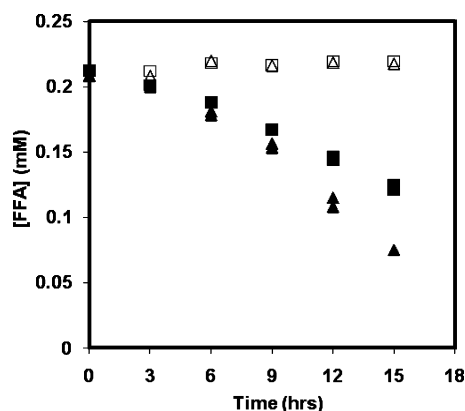


**FIGURE 3.** FFA loss at pH 7 under lamp light in 0.6 mg/L $nC_{60}$, containing 10 mM $NaN_3$ (■), and 10 mM NaCl (▲), and FFA recovery in the corresponding dark control samples [$NaN_3$ (□) and NaCl (△)].

clusters prepared by mixing pure $C_{60}$ with pure water that indicate reaction still occurs in the absence of THF or its byproducts.

An additional experiment was performed in the presence of 10 mM azide ion ($N_3^-$), a $^1O_2$ quencher ($k_d$ ($N_3^-$) = $9 \times 10^8$ M$^{-1}$ s$^{-1}$) (*25*), and compared to that containing 10 mM NaCl to hold ionic strength constant (Figure 3). The FFA loss decreased from 65% in 10 mM NaCl to 40% in 10 mM $NaN_3$ after 15 h of irradiation in lamp light, again supporting $^1O_2$ formation.

Although FFA is a fairly specific indicator for detecting $^1O_2$ (*26*), incomplete quenching of $^1O_2$ in the presence of 10 mM $N_3^-$ suggests the presence of other ROS. To test this hypothesis, nitro blue tetrazolium salt ($NBT^{2+}$) (*27*) was used as a chemical probe for $O_2^{\cdot-}$ where the reaction of $NBT^{2+}$ with $O_2^{\cdot-}$ results in a product that absorbs light at 530 nm (see Figure S1 in the SI). Irradiated $NBT^{2+}$ with and without $nC_{60}$ reveals a slow yet comparable increase in absorbance at $\lambda = 530$ nm over time (after subtracting light attenuation by $nC_{60}$), with a minimal change occurring in the absorbance of dark control samples containing $nC_{60}$ and $NBT^{2+}$, indicating negligible increase in $O_2^{\cdot-}$ production in the presence of $nC_{60}$, and that long irradiation of $NBT^{2+}$ results in some product formation with light absorbance at 530 nm, consistent with past reports (*8, 11*). Indeed, the *Type I* pathway for $nC_{60}$ photoreaction requires an electron donor. This result suggests that the product(s) formed from $nC_{60}$ phototransformation do not serve as electron donors under our experimental conditions. FFA loss in the presence of $N_3^-$, shown in Figure 3, is evidence that $^1O_2$ is not completely quenched by 10 mM $N_3^-$.

Figure 4 compares the photochemical reaction of aqueous $nC_{60}$ (4a) to molecular $C_{60}$ dissolved in ethanol (4b), both under lamp light with FFA present. While the FFA loss was >80% in 1 h by $C_{60}$ in ethanol, only 65% loss occurred after 15 h by $nC_{60}$, indicating that $^1O_2$ production by molecular $C_{60}$ is much more efficient. Although $H_2O$ quenches $^1O_2$ at 3 times the rate of ethanol ($k_d$ ($H_2O$) = $2.5 \times 10^5$ s$^{-1}$ versus $k_d$ (ethanol) = $8 \times 10^4$ s$^{-1}$) (*25*), solvent quenching was not proportional to the decrease ($\gg$ 3 fold) in the FFA loss rate, ruling out the solvent effect as the only factor in the observed differential reactivity. Inspection of the FFA degradation time courses indicates that while the reaction of $C_{60}$ in ethanol followed pseudo first-order kinetics, FFA decay in $nC_{60}$ suspensions displayed a lag period. Indeed, initially heterogeneous species (i.e., nanocrystalline $C_{60}$ and dissolved FFA and $O_2$) were involved in the reaction, and as the reaction proceeded, more products formed with 55% $C_{60}$ loss after 15 h. Our previous work (*9*) has demonstrated that irradiating $nC_{60}$ results in water-soluble products that have currently unknown identi-
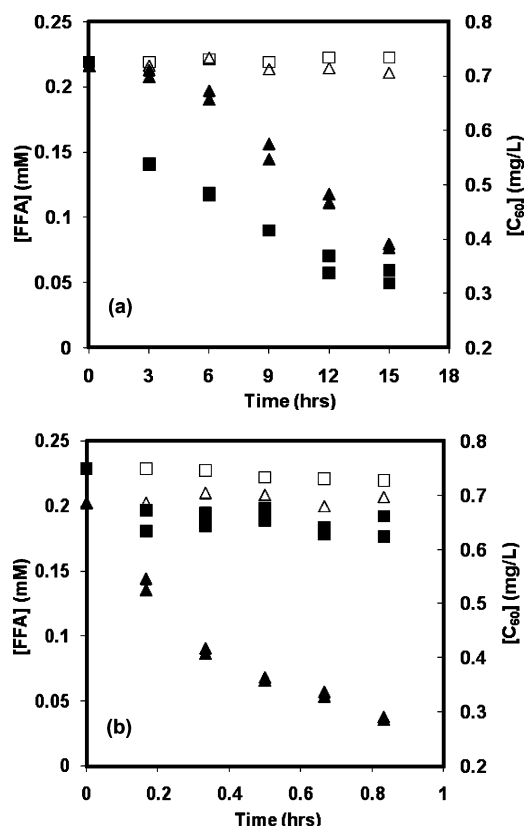
FIGURE 4. FFA (▲) and $C_{60}$ (■) decay in lamp light from (a) an aqueous 0.75 mg/L $nC_{60}$ suspension at pH = 7, and (b) $C_{60}$ dissolved in ethanol, and the recoveries from the corresponding dark control samples [FFA (△) and $C_{60}$ (□)].

ties and may be more photoactive than parent $nC_{60}$, leading to the autocatalytic $^1O_2$ production. The lack of increase in the rate of $C_{60}$ loss while the rate of $^1O_2$ production increased suggests $^3C_{60}$ as a limiting intermediate (12). An additional experiment was performed comparing $nC_{60}$ to rose Bengal (RB), a well-known $^1O_2$ sensitizer (Figure S2). The $^1O_2$ production rate by RB was 7-fold higher than $nC_{60}$ at the same molar concentrations. However, the fact that the $C_{60}$ exists in heterogeneous form strongly suggests that $^1O_2$ production initially occurs via $nC_{60}$.

To test the photoreactivity of the soluble $C_{60}$-decay products, the soluble fractions were isolated, spiked with 0.2 mM FFA, and buffered at pH = 7 for further irradiation. For this, three samples of $nC_{60}$ (initial $[C_{60}] = 0.8$ mg/L) before and after 6 and 9 h of irradiation in the lamp light were centrifuged at 13,000g for 5 h prior to passing the supernatants through 20-nm pore-size membrane filters (Anodisc 25, Whatman, Maidstone, UK). The filtrates were collected and designated as 0-h, 6-h, and 9-h filtrate, respectively. Loss of $C_{60}$ after 6 and 9 h of irradiation were 45% and 50%, respectively. Sequential centrifugation and filtration steps were able to remove 95% of the initial $C_{60}$ mass from each filtrate as determined by toluene extraction and HPLC analysis. The results of FFA loss from the resulting supernatant solutions are shown in Figure 5. The loss of FFA follows the order of 9-h > 6-h > parent $nC_{60}$ > 0-h, with <10% FFA loss in the 0-h filtrate. Some loss in the 0-h filtrate sample may be expected as $C_{60}$ removal via our centrifugation/ filtration method was not 100% complete. All corresponding dark control samples showed no FFA loss (data not shown). A past study has indicated that irradiating $C_{60}$ in nonpolar organic solvents results in insoluble multioxygenated $C_{60}$ products (28). The increasing reactivity (i.e., 0-h < 6-h < 9-h) is consistent with our earlier observation (9) that photo-
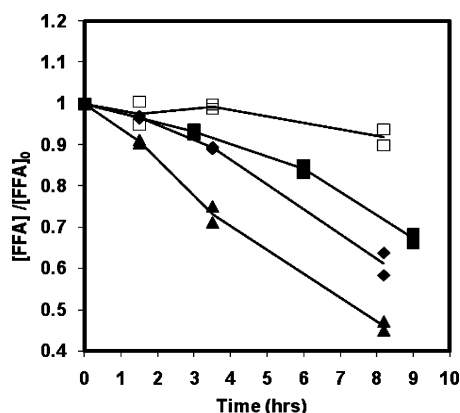


FIGURE 5. Loss of 0.2 mM FFA in lamp light at pH 7 in (■) 0.8 mg/L $nC_{60}$, (□) 0-h filtrate, (♦) 6-h filtrate, and (▲) 9-h filtrate.

products accumulated in the aqueous phase, and shows qualitatively that these water-soluble materials are themselves quite photoreactive, consistent with the lag in FFA decay in Figure 4a.

Previous research (11−13) has indicated that $C_{60}$ loses its intrinsic photoreactivity, including its ability to form ROS (i.e., $^1O_2$ and $O_2^{\cdot-}$), when it is present as aqueous clusters, which seems to conflict with the presented results. For example, another study (11) examined FFA decay under similar solution conditions of FFA/$C_{60}$ (mol/mol) = 120 with lamps emitting light from 350 to 400 nm, compared to ours at FFA/$C_{60}$ = 144 with lamps emitting light from 300 to 410 nm. In this other study, minimal FFA degradation was observed; however, the reported light intensity was 10-fold less (i.e., $5.55 \times 10^{-6}$ versus $6.39 \times 10^{-5}$ einstein $L^{-1}$ $s^{-1}$) and the irradiation time was only 1−2 h compared to our 15-h exposure time. Even under our light conditions, FFA loss was <5% in 2 h of irradiation, and would significantly decrease with decreasing light intensity. Indeed, we show that $^1O_2$ production via $nC_{60}$ is autocatalytic with the initial rate very slow, as the photoproducts clearly increase the rate of $^1O_2$ formation. The loss of $C_{60}$ suggests that the $^1O_2$ produced via $nC_{60}$ reacts with $^3C_{60}$ as previous studies have indicated (15, 16), leading to the photo-oxidation of $C_{60}$. The data presented in Figure 1 a and b strongly support this view as removing $O_2$, the precursor of $^1O_2$, leads to essentially no loss of FFA or $C_{60}$. Another recent study (14) also reports that $^1O_2$ is generated via $nC_{60}$ under pulsed or steady-state UV irradiation at 366 nm by directly detecting $^1O_2$'s characteristic phosphorescence at $\lambda = 1270$ nm. $^1O_2$ photoinduced by $nC_{60}$ cannot be measured indirectly using FFA or spinning trapping chemicals in short-term irradiations (<2 h) as the transformation rate (i.e., dC/dt) of these substances (via reaction with $^1O_2$) is too low, consistent with previous studies (11, 13). As of now, we are not able to distinguish between $^1O_2$ generated by $nC_{60}$ or its photoproducts; the photoproducts, however, likely produce significant $^1O_2$ as time progresses. Finally, it is recognized that significant quenching of $^3C_{60}$ occurs when $C_{60}$ is in clusters as evidenced by Lee et al. (12), however, the quenching is not complete as $^3C_{60}$'s reported half-life in clusters is in the picosecond range, indicating a very low steady-state concentration of $^3C_{60}$ must exist under constant irradiation, leading to $^1O_2$ formation as reported here and by Bilski et al. (14).

Some experiments were performed in sunlight to evaluate the potential environmental rate of $^1O_2$ production from $nC_{60}$. Irradiating FFA alone did not lead to FFA loss in all cases (data not shown). Figure 6a shows FFA loss in 130 and 500 nm diameter $nC_{60}$ cluster suspensions in sunlight. The FFA concentration decreased more rapidly for the 130 nm clusters, indicating the rate of $^1O_2$ production is a function of cluster size. This size-dependency also suggests that as reaction
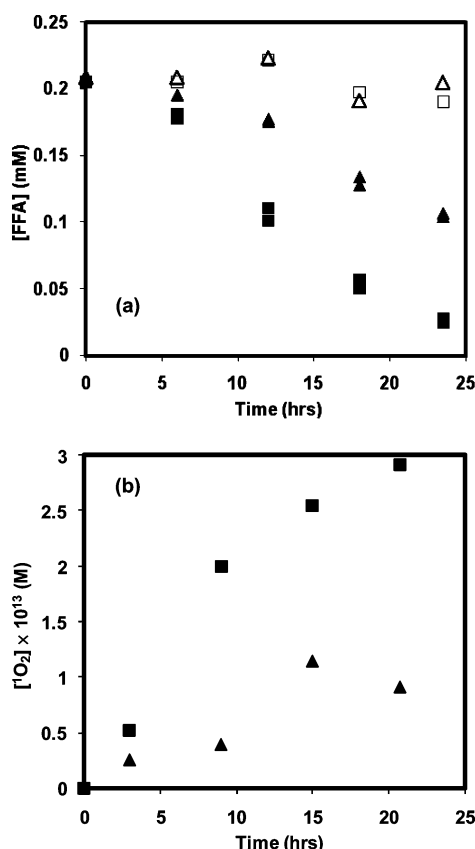
**FIGURE 6. Photochemical production of $^1O_2$ by 130-nm (■) and 500-nm (▲) diameter $nC_{60}$ (1 mg/L) under solar exposure from July 23 to August 11, 2008 at pH = 7, showing (a) FFA loss, and (b) the calculated $[^1O_2]$ in the irradiated samples, and the recovery of FFA in dark control samples [130 nm (□) and 500 nm (△)]. The average solar energy from 300 to 800 nm during irradiation was 502 W m$^{-2}$.**



**FIGURE 7. Estimated $^1O_2$ production by Suwannee River fulvic acid (FA) (▲), $nC_{60}$ (■), and $nC_{60}$ + FA (♦) under solar exposure from July 15 to July 17, 2008 at pH = 7, with initial concentrations of $nC_{60}$ and FA at 5 mg/L. The average solar energy from 300 to 800 nm during irradiation was 525 W m$^{-2}$.**

**TABLE 1. Comparison of $[^1O_2]$ Measured in This Study to Values Reported for Surface Waters**

| water source | sunlight intensity (W/m$^2$) | DOC (mg/L) | $[^1O_2]^0_{ss}$ $^g$ ($\times 10^{14}$ M) | $[^1O_2]^0_{ss}$/DOC ($\times 10^{14}$ M per mg/L) |
|---|---|---|---|---|
| $nC_{60}$ $^a$ | 525 | 5 | 71.1$^{h,i}$ | 14.2$^h$ |
| FA $^a$ | 525 | 2.6 | 5.6$^i$ | 2.1 |
| Swiss surface waters $^b$ | 1000$^f$ | 3.2–13 | 5.9–28$^i$ | 0.8–3.2 |
| municipal wastewaters $^{b,c}$ | 1000$^f$ | 8.6–31 | 11–15$^i$ | 0.3–1.1 |
| U.S. surface and coastal waters $^d$ | 800 | 4–77 | 6–71$^j$ | 0.7–2.9 |
| Dutch surface waters $^e$ | 800 | 8–21 | 0.4–7.6$^j$ | 0.22 |

$^a$ This study. $^b$ Data from Haag et al. (*18*). $^c$ Influents and secondary effluents, and the inflow and outflow of a waste stabilization pond in Switzerland. $^d$ Data from Zepp et al. (*17*). $^e$ Data from Wolff et al. (*29*). $^f$ λ = 280−2800 nm in summer-noon sunlight. $^g$ Corrected to a flat surface water body (*18*). S$_λ$ was calculated at 400 nm for $nC_{60}$. $^h$ Value after 10 h of sunlight irradiation. $^i$ Measured by the FFA method. $^j$ Measured by 2, 5-dimethylfuran (DMF) method using $k_r$ = 6.3 × 10$^8$ M$^{-1}$s$^{-1}$ (*18*).

**TABLE 2. Initial $^1O_2$ Production Rate (0−3 h) under Sunlight Exposure from July 15 to July 17, 2008 at pH = 7 for Initial $nC_{60}$ Concentrations of 1, 5, and 10 mg/L$^a$**

| $[nC_{60}]$ (mg/L) | Δ$[^1O_2]$/Δ$t$ ($\times 10^{13}$ M/h) | Δ$[^1O_2]$/Δ$t$/$[nC_{60}]$ ($\times 10^{13}$ M/h per mg/L) |
|---|---|---|
| 1 | 0.28 | 0.28 |
| 5 | 0.59 | 0.12 |
| 10 | 1.09 | 0.11 |

$^a$ The average solar energy from 300 to 800 nm during the irradiation period was 525 W m$^{-2}$.

proceeds, the observed rate constant for $C_{60}$ loss ($-k_{obs}$) will increase because of the decreased $nC_{60}$ size, although with decreasing concentration, the actual rate (i.e., $-k_{obs}\cdot[C_{60}]$) is expected to continue to decrease (*9*). Although the sunlight intensity varied over the irradiation period, the characteristic lag in FFA decay occurred in sunlight. $^1O_2$ concentrations, calculated with eq 4, are reported in Figure 6b, and the corresponding $C_{60}$ concentrations are shown in Figure S3. The $^1O_2$ concentration increased over time to 3 × 10$^{-13}$ M and 1 × 10$^{-13}$ M after 21 h of sunlight exposure for 130-nm and 500-nm diameter $nC_{60}$ clusters, respectively. The $^1O_2$ concentration increase was not linear with time, and especially for the 130-nm clusters appeared S-shaped, leveling off at longer time periods due to depletion of the substrate concentration (i.e., FFA).

Natural organic matter is important in mediating $^1O_2$ production in natural waters (*17, 18*). Figure 7 compares $^1O_2$ production by 5 mg/L $nC_{60}$ with and without 5 mg/L Suwannee River fulvic acid (FA), and by 5 mg/L FA alone in sunlight. While $[^1O_2]$ values in 5 mg/L FA appeared to be at steady-state at 0.84 × 10$^{-13}$ M, the "non-steady state" concentration of $^1O_2$ in 5 mg/L $nC_{60}$ slowly increased to 8.0 × 10$^{-13}$ M. The addition of 5 mg/L FA to 5 mg/L $nC_{60}$ had no effect on $[^1O_2]$ over time. Recall, eq 3 is valid for steady-state conditions: $[^1O_2]_{ss}$ calculated in FA samples with eq 3 is 0.85 × 10$^{-13}$ M compared to 0.84 × 10$^{-13}$ M calculated with eq 4, indicating the utility of eq 4. Normalizing $[^1O_2]$ by the sensitizer DOC content (2.63 mg/L for FA and 5 mg/L for $nC_{60}$), correcting the rate measured in test tubes to that expected for flat open surface waters (i.e., a factor of 1.5 lower) (*18*) and correcting for light attenuation (i.e., eq 5)
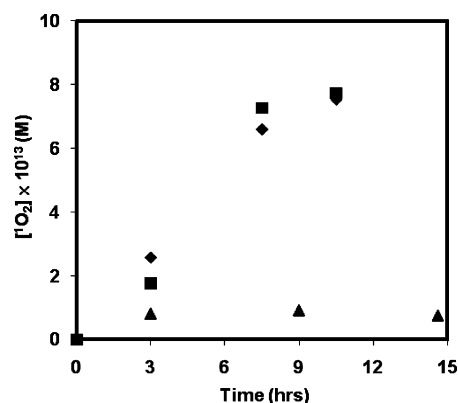
(*18*) gives 2.1 × 10$^{-14}$ and 14.2 × 10$^{-14}$ M $^1O_2$ per mg/L DOC for FA and $nC_{60}$, respectively. Table 1 compares $[^1O_2]_{t = 10 h}$ obtained in this study for $nC_{60}$ to values of $[^1O_2]_{ss}$ determined for various surface waters (*17, 18, 29*). The comparison shows that while $[^1O_2]$ induced by FA is within the typical values reported for surface waters, $[^1O_2]$ induced by $nC_{60}$ is 4−65 fold higher.

Table 2 reports initial $[^1O_2]$ accumulation rates for 1, 5, and 10 mg/L $nC_{60}$ suspensions. Because $C_{60}$ intermediates affect $^1O_2$ levels at longer irradiation times, an initial rate study was performed to compare $^1O_2$ accumulation rates

after a short sunlight exposure time of 3 h. The longer term accumulation of $^1O_2$ for these $nC_{60}$ suspensions is presented in Figure S5. The initial rate ($\Delta[^1O_2]/\Delta t$) increased from 0.28 $\times 10^{-13}$ to 1.09 $\times 10^{-13}$ M h$^{-1}$ with increasing $nC_{60}$ concentration from 1 to 10 mg/L. Dividing the initial rate by the $nC_{60}$ concentration, however, gives the accumulation per mg/L $C_{60}$-added and reveals a decline in accumulation at the high initial $nC_{60}$ concentrations. Both increasing light attenuation (inner-filter affect) and increasing quenching of $^3C_{60}$ and $^1O_2$ by $C_{60}$ may occur with increasing $nC_{60}$ concentration (10, 30).

This and our previous study (9) suggest that although $C_{60}$'s photoreactivity drastically decreases when it occurs in aqueous aggregates, it does occur in sunlight within an environmentally relevant time scale forming products that are more photoactive and that further catalyze $^1O_2$ production. Additional research is needed to identify these photoproducts and their environmental impacts, including ROS generation.

## Acknowledgments

## Supporting Information Available

Additional information on the sources of chemicals, $C_{60}$ solution preparation procedures, detection of superoxide anion, comparison of the $^1O_2$ production by $nC_{60}$ and RB, losses of $C_{60}$ from 130-nm and 150-nm diameter $nC_{60}$ in the presence of 0.2 mM FFA in sunlight, $^1O_2$ production by 1 mg/L $nC_{60}$ at pH = 5, 7, and 9 in sunlight, and accumulation of $^1O_2$ in 1, 5, and 10 mg/L $nC_{60}$ in longer irradiation time in sunlight. This material is available free of charge via the Internet at http://pubs.acs.org.

## Literature Cited

(1) The Project of Emerging Nanotechnologies. An inventory of nanotechnology-based consumer products currently on the market; http://www.nanotechproject.org/inventories/consumer/.

(2) Oberdorster, E. Manufactured nanomaterials (fullerene, $C_{60}$) induce oxidative stress in the brain of juvenile largemouth bass. *Environ. Health Perspect.* **2004**, *112*, 1058–1062.

(3) Henry, T.; Menn, F. M.; Fleming, J. T.; Wilgus, J.; Compton, R. N.; Sayler, G. S. Attributing effects of aqueous $C_{60}$ nano-aggregates to tetrahydrofuran decomposition products in larval zebrafish by assessment of gene expression. *Environ. Health Perspect.* **2007**, *115*, 1059–1065.

(4) Jafvert, C. T.; Kulkarni, P. P. Buckminsterfullerene's ($C_{60}$) octanol-water partition coefficient ($K_{ow}$) and hypothetical aqueous solubility. *Environ. Sci. Technol.* **2008**, *42*, 5945–5950.

(5) Deguchi, S.; Alargova, R. G.; Tsujii, K. Stable dispersion of fullerenes, $C_{60}$, and $C_{70}$, in water. Preparation and characterization. *Langmuir* **2001**, *17*, 6013–6017.

(6) Foote, C. S. Definition of type I and II photosensitized oxidation. *Photochem. Photobiol.* **1991**, *54*, 659.

(7) Arbogast, J. W.; Foote, C. S.; Kao, M. Electron transfer to triplet $C_{60}$. *J. Am. Chem. Soc.* **1992**, *114*, 2277–2279.

(8) Yamakoshi, Y.; Umezawa, N.; Ryu, A.; Arakane, K.; Miyata, N.; Goda, Y.; Masumizu, T.; Nagano, T. Active oxygen species generated from photoexcited fullerene ($C_{60}$) as potential medicines: $O_2^{-\cdot}$ versus $^1O_2$. *J. Am. Chem. Soc.* **2003**, *125*, 12803–12809.

(9) Hou, W.-C.; Jafvert, C. T. Photochemical transformation of aqueous $C_{60}$ clusters in sunlight. *Environ. Sci. Technol.* **2009**, *43*, 362–367.

(10) Arbogast, J. W.; Darmanyan, A. P.; Foote, C. S.; Rubin, Y.; Diederich, F. N.; Alvarez, M. M.; Anz, S. J.; Whetten, R. L. Photophysical properties of $C_{60}$. *J. Phys. Chem.* **1991**, *95*, 11–12.

(11) Lee, J.; Fortner, J. D.; Hughes, J. B.; Kim, J. Photochemical production of reactive oxygen species by $C_{60}$ in the aqueous phase during UV irradiation. *Environ. Sci. Technol.* **2007**, *41*, 2529–2535.

(12) Lee, J.; Yamakoshi, Y. D.; Hughes, J. B.; Kim, J. Mechanism of $C_{60}$ photoreactivity in water: Fate of triplet state and radical anion and production of reactive oxygen species. *Environ. Sci. Technol.* **2008**, *42*, 3459–3464.

(13) Hotze, E. M.; Labille, J.; Alvarez, P.; Wiesner, M. R. Mechanisms of photochemistry and reactive oxygen production by fullerene suspensions in water. *Environ. Sci. Technol.* **2008**, *42*, 4175–4180.

(14) Bilski, P.; Zhao, B.; Chignell, C. F. Singlet oxygen phosphorescence photosensitized in nano-aggregates of $C_{60}$ buckminsterfullerene is insensitive to solvent and quenchers and strongly red-shifted indicating highly polarizable interior. *Chem. Phys. Lett.* **2008**, *458*, 157–160.

(15) Juha, L.; Hamplova, V.; Kodymova, J.; Spalek, O. Reactivity of fullerene with chemically generated singlet oxygen. *J. Chem. Soc. Chem. Commun.* **1994**, 2437–2438.

(16) Schuster, D. I.; Baran, P. S.; Hatch, R. K.; Khan, A. U.; Wilson, S. R. The role of singlet oxygen in the photochemical formation $C_{60}O$. *J. Chem. Soc. Chem. Commun.* **1998**, 2493–2494.

(17) Zepp, R. G.; Wolfe, N. L.; Baughman, G. L.; Hollis, R. C. Singlet oxygen in natural waters. *Nature* **1977**, *267*, 421–423.

(18) Haag, W. R.; Hoigne, J. Singlet oxygen in surface waters. 3. Photochemical formation and steady-state concentration in various types of waters. *Environ. Sci. Technol.* **1986**, *20*, 341–348.

(19) Zepp, R. G.; Baughman, G. L.; Schlotzhauer, P. F. Comparison of photochemical behavior of various humic substances in water: I. Sunlight induced reactions of aquatic pollutants photosensitized by humic substances. *Chemosphere* **1981**, *10*, 109–117.

(20) Tokuyama, H.; Yamago, S.; Nakamura, E.; Shiraki, T.; Sugiura, Y. Photoinduced biochemical activity of fullerene carboxylic acid. *J. Am. Chem. Soc.* **1993**, *115*, 7918–7919.

(21) Kamat, J. P.; Devasagayam, T. P. A.; Priyadarsini, K. I.; Mohan, H. Reactive oxygen species mediated membrane damage induced by fullerene derivatives and its possible biological implications. *Toxicology* **2000**, *155*, 55–61.

(22) Haag, W. R.; Hoigne, J.; Gassmann, E.; Braun, A. M. Singlet oxygen in surface waters - Part I: Furfuryl alcohol as a trapping agent. *Chemosphere* **1984**, *13*, 631–640.

(23) Tratnyek, P. G.; Hoigne, J. Oxidation of substituted phenols in the environment: A QSAR analysis of rate constants for reaction with singlet oxygen. *Environ. Sci. Technol.* **1991**, *25*, 1596–1604.

(24) Zepp, R. G.; Schlotzhauer, P. F.; Sink, R. M. Photosensitized transformations involving electronic energy transfer in natural waters: Role of humic substances. *Environ. Sci. Technol.* **1985**, *19*, 74–81.

(25) Wilkinson, F.; Helman, W. P.; Ross, A. B. Rate constants for the decay and reactions of the lowest electronically excited singlet state of molecular oxygen in solution-An expanded and revised compilation. *J. Phys. Chem. Ref. Data* **1995**, *24*, 663–1021.

(26) Maurette, M.-T.; Oliveros, E.; Infelta, P. P.; Ramsteiner, K.; Braun, A. M. 68. Singlet oxygen and superoxide: Experimental differentiation and analysis. *Helv. Chim. Acta* **1983**, *66*, 722–733.

(27) Bleski, B. H.; Shiue, G. G.; Bajuk, S. Reduction of nitro blue tetrazolium by $CO_2^-$ and $O_2^-$ radicals. *J. Phys. Chem.* **1980**, *84*, 830–833.

(28) Taylor, R.; Parsons, J. P.; Avent, A. G.; Rannard, S. P.; Dennis, T. J.; Hare, J. P.; Kroto, H. W.; Walton, D. R. Degradation of $C_{60}$ by light. *Nature* **1991**, *351*, 277.

(29) Wolff, C. J. M.; Halmans, M. T. H.; Van der Heijde, H. B. The formation of singlet oxygen in surface waters. *Chemosphere* **1981**, *10*, 59–62.

(30) Kamat, P. V.; Dimitrijevic, N. M. Triplet excited state behavior of fullerenes: pulse radiolysis and laser flash photolysis of $C_{60}$ and $C_{70}$ in benzene. *J. Phys. Chem.* **1992**, *96*, 4811–4814.

ES900624S